LOAN DOCUMENT

PHOTOGRAPH THIS SHEET

LEVEL

INVENTORY

0

DTIC ACCESSION NUMBER

Kinetics of Supercritical Water Oxidation
QR. Oct 1 - Dec 31, 1996

DOCUMENT IDENTIFICATION

1996

DISTRIBUTION STATEMENT A
Approved for public release;
Distribution Unlimited

DISTRIBUTION STATEMENT

ACCESSION FOR
NTIS GRA&I ☒
DTIC TRAC ☐
UNANNOUNCED ☐
JUSTIFICATION

BY

DISTRIBUTION/

AVAILABILITY CODES

DISTRIBUTION	AVAILABILITY AND/OR SPECIAL	
A-1		

DISTRIBUTION STAMP

DATE ACCESSIONED

DATE RETURNED

19980710 081

DATE RECEIVED IN DTIC

REGISTERED OR CERTIFIED NUMBER

PHOTOGRAPH THIS SHEET AND RETURN TO DTIC-FDAC

HANDLE WITH CARE

DTIC FORM 70A JUN 90

DOCUMENT PROCESSING SHEET

PREVIOUS EDITIONS MAY BE USED UNTIL STOCK IS EXHAUSTED.

LOAN DOCUMENT

REPORT DOCUMENTATION PAGE

Form Approved
OMB No. 074-0188

1. AGENCY USE ONLY (Leave blank)	2. REPORT DATE 1996	3. REPORT TYPE AND DATES COVERED Quarterly Report, Oct 1 - Dec 31, 1996

4. TITLE AND SUBTITLE

Kinetics of Supercritical Water Oxidation

5. FUNDING NUMBERS

N/A

6. AUTHOR(S)

S.F. Rice, R.R. Steeper, R.G. Hanush. J.D. Aiken, E. Croiset, J.W. Tester, K. Brezinsky

7. PERFORMING ORGANIZATION NAME(S) AND ADDRESS(ES)

Sandia National Laboratories
Combustion Research Facility

8. PERFORMING ORGANIZATION REPORT NUMBER

Case 8610.000

9. SPONSORING / MONITORING AGENCY NAME(S) AND ADDRESS(ES)

SERDP
901 North Stuart St. Suite 303
Arlington, VA 22203

10. SPONSORING / MONITORING AGENCY REPORT NUMBER

N/A

11. SUPPLEMENTARY NOTES

This work was supported in part by SERDP. The United States Government has a royalty-free license throughout the world in all copyrightable material contained herein. All other rights are reserved by the copyright owner.

12a. DISTRIBUTION / AVAILABILITY STATEMENT

Approved for public release: distribution is unlimited

12b. DISTRIBUTION CODE

A

13. ABSTRACT ***(Maximum 200 Words)***

This project consists of experiments and theoretical modeling designed to improve our understanding of the detailed chemical kinetics of supercritical water oxidation processes. The objective of the four-year project is to develop working models that accurately predict the oxidation rates and mechanisms for a variety of key organic species over the range of temperatures and pressures important for industrial applications. Our examination of reaction kinetics in supercritical water undertakes in situ measurements of reactants, intermediates, and products using optical spectroscopic techniques, primarily Raman spectroscopy. Our focus is to measure the primary oxidation steps that occur in the oxidation of methanol, higher alcohols, methylene chloride, aromatics, and some simple organic compounds containing nitro groups. We are placing special emphasis on identifying reaction steps that involve hydroxyl radicals, hydroperoxyl radicals, and hydrogen peroxide. The measurements are conducted in two optically accessible reactors located at Sandia's Combustion Research Facility (CRF), the supercritical flow reactor (SFR) and the supercritical constant volume reactor, designed to operate at temperatures and pressures up to 600 ^{0}C and 500 MPa. The combination of these two reactors permits reaction rate measurements ranging from 0.1 s to many hours.

14. SUBJECT TERMS

Kinetics, Supercritical water oxidation, Supercritical flow reactor, SERDP

15. NUMBER OF PAGES

21

16. PRICE CODE N/A

17. SECURITY CLASSIFICATION OF REPORT	18. SECURITY CLASSIFICATION OF THIS PAGE	19. SECURITY CLASSIFICATION OF ABSTRACT	20. LIMITATION OF ABSTRACT
unclass.	unclass.	unclass.	UL

Kinetics of Supercritical Water Oxidation

SERDP Compliance Technical Thrust Area

Quarterly Report

Sandia National Laboratories
Combustion Research Facility
Case 8610.000

Principal Investigator:	Steven F. Rice, Sandia
Project Associates, Sandia:	Richard R. Steeper Russell G. Hanush, Jason D. Aiken,
Visiting Scientist:	Eric Croiset, CNRS Orléans
University Collaborators:	Jefferson W. Tester, MIT Kenneth Brezinsky, U. of Illinois, Chicago Irvin Glassman, Princeton University
Project Manager:	Donald R. Hardesty
Reporting Period:	October 1 – December 31, 1996

Project description

This project consists of experiments and theoretical modeling designed to improve our understanding of the detailed chemical kinetics of supercritical water oxidation (SCWO) processes. The objective of the five-year project is to develop working models that accurately predict the oxidation rates and mechanisms for a variety of key organic species over the range of temperatures and pressures important for industrial applications. Our examination of reaction kinetics in supercritical water undertakes *in situ* measurements of reactants, intermediates, and products using optical spectroscopic techniques, primarily Raman spectroscopy. Our focus is to measure the primary oxidation steps that occur in the oxidation of methanol, higher alcohols, methylene chloride, aromatics, and some simple organic compounds containing nitro groups. We are placing special emphasis on identifying reaction steps that involve hydroxyl radicals, hydroperoxyl radicals, and hydrogen peroxide. The measurements are conducted in two optically accessible reactors located at Sandia's Combustion Research Facility (CRF), the supercritical flow reactor (SFR) and the supercritical constant volume reactor (SCVR), designed to operate at temperatures and pressures up to 600°C and 500 MPa. The combination of these two reactors permits reaction rate measurements ranging from 0.1 s to many hours.

The work conducted here continues the experimental approach from earlier years of this SERDP-funded project by extending measurements on key oxidant species and expanding the variety of experimental methods, primarily spectroscopic in nature, that can be used to examine reactions at SCWO conditions. Direct support is provided to the project by collaborators at MIT and Princeton who are contributing to model development for phenol, other aromatics, and halogenated species. These researchers are examining these processes using more conventional sample-and-quench methods.

Executive Summary of Progress this Period

Programmatic

This quarter, there were a number of presentations at technical conferences highlighting the results of this project. Among these was a presentation at the Second Annual SERDP Symposium. Preparation for these meetings consumed a significant amount of effort this quarter. The work was well received, and as a result, a number of recipients have been added to the mailing list for these Quarterly Reports. Some of this is the result of growing interest regarding the application of SCWO to the destruction of hydrolysate from the neutralization of chemical warfare agents.

Jessica Wickham, a Co-op student from Cornell University completed her work as a laboratory assistant at Sandia for the Fall Semester. She will be returning for the summer of 1997 for the second half of the Co-op program. In addition, the project is fortunate that Eric Croiset, out post-doctoral visiting scientist form CNRS Orléans, has chosen to extend his stay at Sandia for several more months through the spring of 1997.

Presently, this project is subject to a $50K DoD holdback for FY1997. SERDP program management was not certain that these funds would be restored FY97. Through consultation with the SERDP program management, Sandia has decided to postpone work on the incorporation of chlorinated species into the C,H,O oxidation description.

Alcohol oxidation

Analysis of an elementary reaction model for the oxidation of methanol in supercritical water has revealed some interesting predictions regarding the interpretation of oxidation reaction kinetics using pseudo-first-order rate constants. This analysis has prompted Sandia and MIT to undertake a series of experiments on the oxidation of methanol under identical conditions and to interpret these

experiments solely in terms of the conversion percentage as a function of time. These "identical conditions" experiments are necessary after it was realized through model analysis of methanol oxidation in supercritical water that the pseudo-first-order description of the oxidation kinetics could lead to serious interpretation inconsistencies.

We have initiated a series of measurements on ethanol to round out our description of small alcohol reactivity. These data will fit in well with work being conducted by Prof. Michael Klein's group at the University of Delaware, Dept. of Chemical Engineering, on the translation of kinetics lumping models from being species-lumped to being reaction-lumped. The University of Delaware work is supported through the Army Research Office. The combination of Sandia's experimental results and the Delaware model development is an excellent opportunity for both groups to leverage their efforts on SCWO fundamental kinetics for DoD technology development applications.

CO/CO_2 water-gas shift chemistry

The maximum pressure of the SCVR has been extended to 60 MPa (8700 psi) and experimental data needed to quantify the homogeneous rate of the water-gas shift in supercritical water have been obtained. The improvements have also allowed these data to be extended to 520 °C. In addition, the new measurements on a "cleaned-up" reactor have significantly reduced the scatter in the lower temperature data set that we have reported earlier.

N_2O thermal decomposition

We have completed the experimental plan and system modifications to the SCVR required to handle N_2O feeds. Preliminary experiments indicate that this system will work well for measuring the conversion of N_2O to N_2 (and O_2) in the presence of supercritical water and reactants such as NH_3. Experiments have been initiated to determine the conversion rate of N_2O in the lower temperature SCWO range of 400 – 520 °C. This is the first key experiment needed to determine parameters for the removal of NO_x from SCWO systems during processing of energetic materials. Our initial observation is that the conversion rate of N_2O to O_2 and N_2 is enhanced by about one order of magnitude in supercritical water relative to an extrapolation to lower temperature of the well-established gas phase high-pressure limit at > 700 °C.

Massachusetts Institute of Technology, Department of Chemical Engineering

The initial attempt to compare data obtained independently at MIT and Sandia on the rate of methanol oxidation showed that under identical operating conditions

Sandia consistently observed a higher conversion of methanol. Comparing the data on an assumed 1st-order Arrhenius plot reveals that the difference in the apparent rate corresponds to a potential temperature measurement mismatch in the reactors of approximately 15 °C. As a result of this observation, during this quarter we installed a new preheating system to improve our ability to preheat the oxidant and organic feeds prior to mixing at the reactor head.

Work has continued on the analysis of the data obtained previously on methylene chloride (CH_2Cl_2) hydrolysis with emphasis placed on modeling solvent effects. As reported last quarter, the loss of polarity of water as it is heated through the critical point should have a debilitating effect on the ionic-based CH_2Cl_2 hydrolysis reaction because of the decreased stability of the polar transition state complex. Thus far, the calculations continue to be in good agreement with what is expected and has been observed experimentally.

Princeton University, Mechanical and Aerospace Engineering Department

Kinetics modeling of the pyrolysis and oxidation of aromatic species in the intermediate temperature range has produced a fairly complete description of anisole pyrolysis. Work this quarter has focused on the subsequent oxidation chemistry converting cyclopentadiene to smaller hydrocarbons and radicals, characterizing the ring break-up and the formation of the second equivalent of CO. Melissa Pecullan is writing her doctoral thesis. Major parts of her work, including the data collection and reaction mechanism development of anisole and phenol pyrolysis and oxidation at intermediate temperatures derives from the collaboration with Sandia through this SERDP project.

Future work

Experimental efforts at Sandia next quarter will be devoted primary to the completion of the ethanol oxidation data set and the extension of the N_2O measurements to a reacting system. Much of the effort will also be directed at completing several papers to be submitted to the literature. These include our hydrogen peroxide thermal decomposition work reported in the last quarterly report, and completion of the water-gas shift and alcohol oxidation papers. The work at Princeton will be focused primarily on the completion of Melissa Pecullan's doctoral thesis. Work at MIT will continue the benzene oxidation data collection and a final resolution of the joint measurements with Sandia.

Publications and presentations

Presentations
"The Effect of Water Concentration on Water-Gas Chemistry in Supercritical Water" Steven F. Rice and Richard R, Steeper. 3rd Conference on Advanced Oxidation Technologies, Cincinnati OH, 10/26/96 – 10/29/96.

"Technology Development Progress in Supercritical Water Oxidation" Steven F. Rice. 1996 Pacific Conference on Chemistry and Spectroscopy", San Francisco CA, 10/30/96 – 11/2/96.

"The Role of Peroxides in Supercritical Water Oxidation", Steven F. Rice. 2nd Annual SERDP Symposium, Tysons Corner VA, 11/20/96 – 11/22/96.

"Reaction Kinetics in Supercritical Water: Raman Spectroscopic Methods and Elementary Modeling" Steven F. Rice, MIT Energy Laboratory Seminar, Cambridge MA, 11/6/96.

Papers and reports
"Raman Spectroscopic Measurement of Oxidation in Supercritical Water. II. Conversion of Isopropanol to Acetone" Thomas B. Hunter, Steven F. Rice, and Russell G. Hanush, *Industrial and Engineering Chemistry Research,* **35,** 3984 3990, 1996.

"Kinetic Investigation of the Oxidation of Naval Excess Hazardous Materials in Supercritical Water for the Design of a Transpiration - Wall Reactor." Rice, S.F., Hanush, R.G., Hunter, T.B., Steeper, R.R., Aiken, J.D., Croiset, E., and LaJeunesse, C.A. Sandia Report. SAND97-8219.

Detailed Summary of Technical Progress this Period

Sandia Combustion Research Facility

Alcohol oxidation

Interpretation of methanol rate constants
We have conducted Chemkin calculations using a modified version of the GRI 1.2 mechanism to explore the variation in the effective first-order rate constant as a function of initial reactant concentration and extent of conversion. Details of this modification are presented in this project's January – March 1996 quarterly progress report. Essentially, the only reaction that was added to the original GRI 1.2 reaction scheme is the direct reaction of HO_2 with methanol. This reaction is absent in the

GRI scheme, but is key to properly describing our experimental results. These calculations were performed at the 500 °C and 24.1 MPa for varying initial feed mole fractions ranging from 10^{-2} to as low as 10^{-5}. The fuel equivalence ratio was 0.75, such that the conditions have ample oxygen to complete the reaction.

Figure 1 shows the results of these calculations. At high feed concentration (10^{-2} mole fraction) there is a relatively short induction period followed by the reaction of a little over two orders of magnitude of the feed that can be accurately approximated as being first order in methanol concentration. These two characteristic reaction stages are illustrated by a straight line on the plot and its extrapolation to an induction time, τ, of approximately 0.4 s. At lower feed concentrations, the induction time increases and approaches 1.5 s prior to the period where the kinetics are dominated by a first-order reaction.

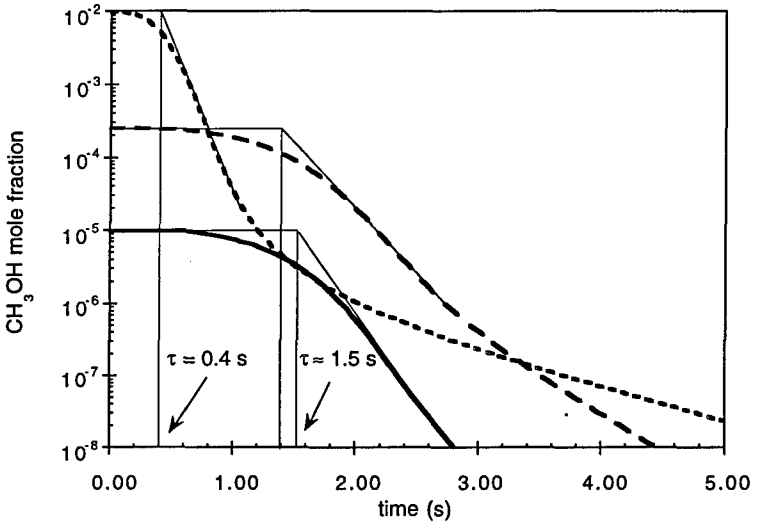

Figure 1 Predicted concentration of methanol as a function of time for different initial feed conditions at 500 °C and 24.1 MPa. Initial mole fractions are 1.0×10^{-2} (dotted line), 2.5×10^{-4} (dashed line), and 1.0×10^{-5} (solid line).

A first-order analysis of the concentration of methanol in samples taken from a reacting flow, described by

$$-\ln (C/C_o)/t = k_{eff} \quad (1)$$

(where C and C_o are the measured and initial concentrations respectively, t is the reactions time, and k_{eff} is the effective first-order rate constant) will produce very different values for k_{eff} when evaluated for different feed concentrations and net

conversions. For example, feeds at 10^{-2} mole fraction and C/C_o = 0.5, yields k_{eff} = 1.73 s^{-1}, but at C/C_o =0.1 k_{eff} = 3.68 s^{-1} and for C/C_o =0.01, (99% conversion) k_{eff} = 5.38 s^{-1}. However, in the case of a more dilute feed (e.g. a mole fraction of 0.025), these same three conversions result in rate constants of 0.52 s^{-1}, 1.16 s^{-1}, and 1.84 s^{-1}. Calculations that are not shown here indicate that this discrepancy becomes more severe as temperature is lowered to 450 °C and below.

This analysis of the behavior of methanol oxidation as a function of feed concentration has produces two key observations that have a direct impact concerning the comparison of pseudo-first-order rate constants for different experiments. The first observation is that data taken for different conversions for a given fixed initial feed concentration will not produce the same rate constant due to the presence of an induction time in the reaction. The second observation is that there is a significant variation in the induction time as a function of feed concentration. This analysis illustrates a critical consideration that had been overlooked previously when comparing effective rate constants reported for oxidation results obtained in the MIT system, the Sandia system, or any other laboratory.

The induction time originates from the slower reaction rate associated with HO_2 + CH_3OH => (CH_2OH or CH_3O) + H_2O_2 which dominates the fuel consumption at early time. The "first order" part of the reaction is dominated by OH + CH_3OH, but is rate controlled by the dissociation of H_2O_2 to supply OH. The H_2O_2 is accumulated during the chain branching induction period. The chain branching process depends on both the concentration of O_2 and on the concentration of CH_3OH and therefore, at constant equivalence ratio, it is a function of fuel mole fraction.

Ethanol oxidation

Understanding the oxidation rate of ethanol in supercritical water oxidation systems is important for several reasons. First it provides a link between the now well-established methanol reaction pathway and the kinetics of larger alcohols for which we have already reported extensive data. A second reason is that because it is one of the more reactive species we have examined, it may be well suited as an initiating fuel. It can be purchased at very low grade and therefore can result in significant operational savings for SCWO applications for feeds that have relatively low heating values. A third reason is that this suite of small alcohols — methanol, ethanol, and i- and n-propanol — is an ideal test system for examining the effect of the presence of a small amount of a reactive compound on the overall oxidation rate of more robust species.

This quarter we initiated a series of experiments on ethanol oxidation using the SFR equipped with Raman spectroscopic diagnostics. Only preliminary results will be presented here. Figure 2 shows a Raman spectrum of the 890 cm^{-1} feature of ethanol in supercritical water at 245 MPa (3550 psi) and 430 °C. Figure 3 shows the spectrum in the same region in the presence of oxygen after 3.5 s of reaction time.

Essentially all of the ethanol is consumed, however there is still an easily measured asymmetrical feature reflecting the presence of an intermediate.

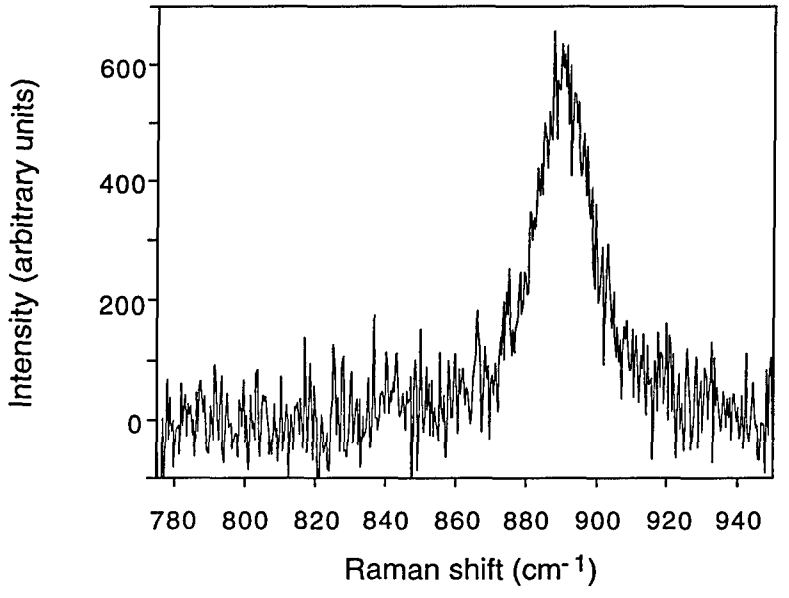

Figure 2 Raman spectrum of ethanol in supercritical water at 24.5 MPa and 430 °C in the 800 – 900 cm^{-1} region.

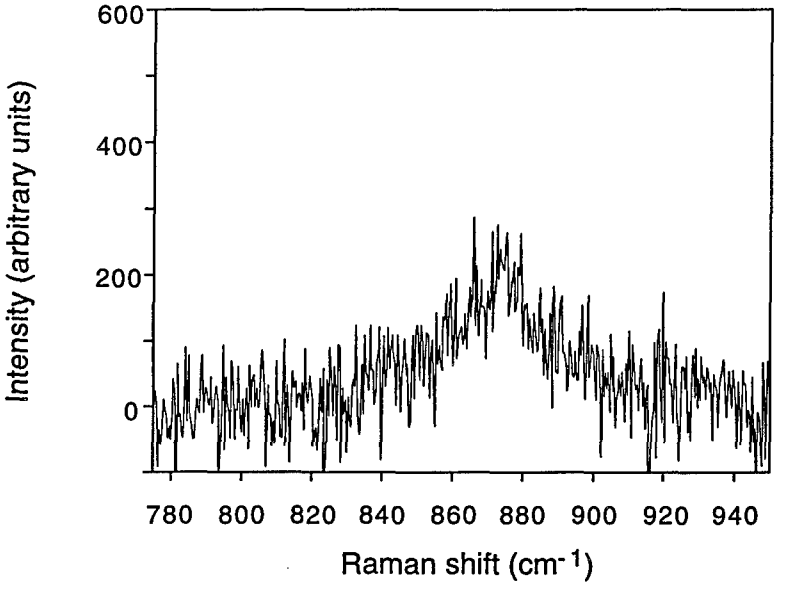

Figure 3 Raman spectrum of a feature at 879 cm^{-1} produced during the oxidation of ethanol.

We believe that the feature at 879 cm^{-1} is actually two bands, one at 879 cm^{-1} and the other at about 850 cm^{-1}. These may be may be due to hydrogen peroxide that is accumulated in the system as a transient and not due to a carbon-containing species. However, more measurements will need to be done to evaluate this and to compare with our n-propanol observations.

CO/CO_2 water-gas shift chemistry

The maximum pressure of the SCVR has been extended to 60.0 MPa (8700 psi). Despite this higher pressure, we have been able to maintain the previous temperature limit of 520 °C. This has permitted us to extend data obtained at 480 °C into the higher density region, above the critical density of water. We have also obtained data at 520 °C as well. Fifteen additional data points were collected at 410 °C. The 410°C data we collected previously are of low quality due to an accumulation of deposits that form on the windows over time. The final set of data needed to produce a quantitative picture of the rate of the homogeneous water-gas shift reaction in supercritical water has been obtained.

Figures 4 and 5 show plots of the complete set of measurements evaluated using a simple first-order rate constant to describe the reaction rate. The additional points obtained this quarter at higher pressure show that the approximately exponential dependence on water density continues to higher densities than had been previously measured. The simple first-order picture is a useful first step to interpreting the data, but it tends to mask some of the complexity of the data. See discussion of Figure 6 below.

In Figure 6, the results of conversion of CO to CO_2 over a wide pressure range at 450 °C are shown. Note that at high pressure the reaction appears to proceed according to nearly first-order kinetics with respect to CO concentration. At pressures below 6000 psi, however, there is an initial loss of 10-20% of the CO before a slower first-order process is established. This has made defining a first order rate constant for these lower-pressure data problematic. We have chosen to discard the early time data in these runs and have used the later-time first-order reaction rate to calculate a k_{eff}.

The presence of this initial rapid loss of CO at low and intermediate pressures suggests that the process that is being measured in this reactor is more complicated than can be expressed using a simple first order expression. Specifically, it may be likely that these lower pressure data are characteristic of a different mechanism, perhaps dominated by surface-catalysis by the reactor itself.

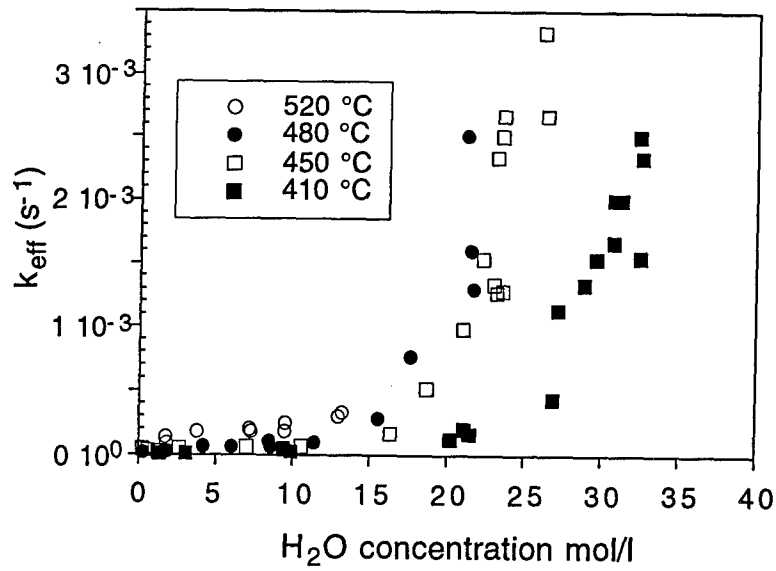

Figure 4 CO conversion rate constants including the new data at 520 °C. New data at 410 °C, 450 °C, and 480 °C are at 33 mol/l, 26 mol/l, and 21 mol/l respectively.

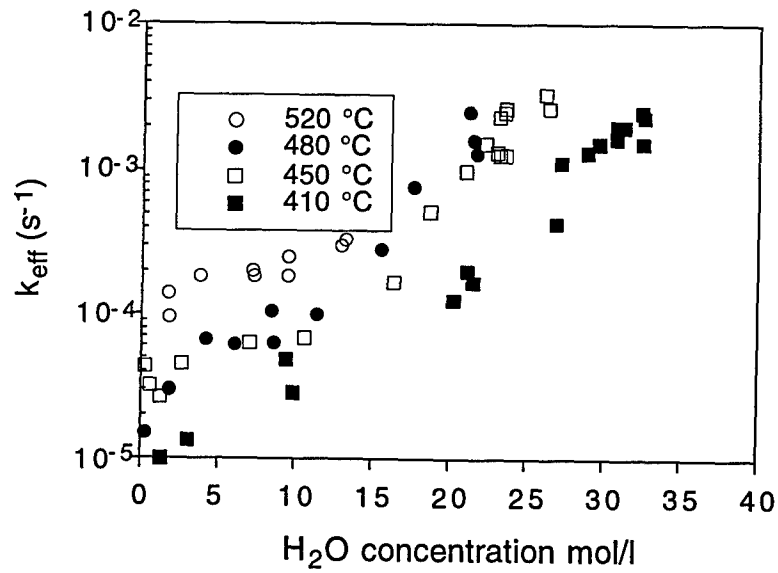

Figure 5 The same data in Figure 4 replotted on a semi-log plot.

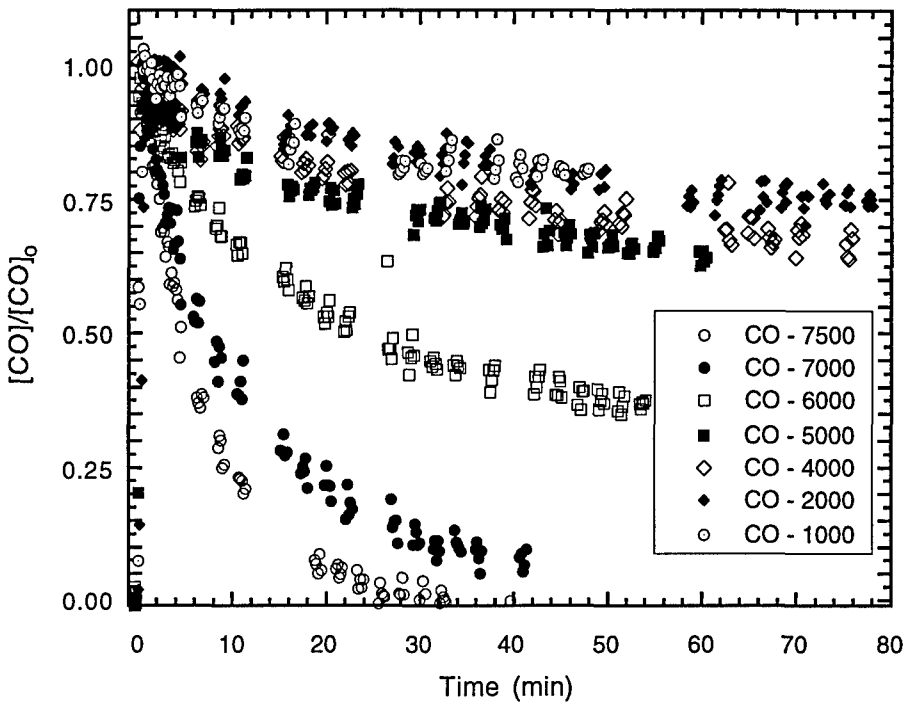

Figure 6 Plot of CO conversion vs. time at a number of pressures (psi) at 450 °C

N_2O thermal decomposition

During this quarter, we have completed the experimental plan and system modifications to the SCVR to handle N_2O feeds. Preliminary experiments indicate that this system will work well for measuring the conversion of N_2O to N_2 (and O_2) in the presence of supercritical water and other reactants such as NH_3. Experiments have been initiated to determine the conversion rate of N_2O in supercritical water in the temperature range of 400 - 510 °C. This is the first experiment needed to determine the parameters for the removal of NO_x from the system. Figure 7 shows a spectrum of the 1285 cm^{-1} Raman feature of N_2O that was used to monitor the N_2O concentration as a function of time.

Our initial observation is that the conversion rate of N_2O to O_2 and N_2 is somewhat enhanced in supercritical water relative to an extrapolation to lower pressure of the higher temperature gas phase high-pressure limit. A prediction for the rate constant for the decomposition of N_2O in supercritical water at 510 °C can be obtained by extrapolation of the high pressure limit reported by Johnsson et. al. (Johnsson, *et al.*, 1992). They report an effective rate constant for this reaction as

$$k_{eff} = 7.2 \times 10^9 \exp(-28250/T) \qquad (2)$$

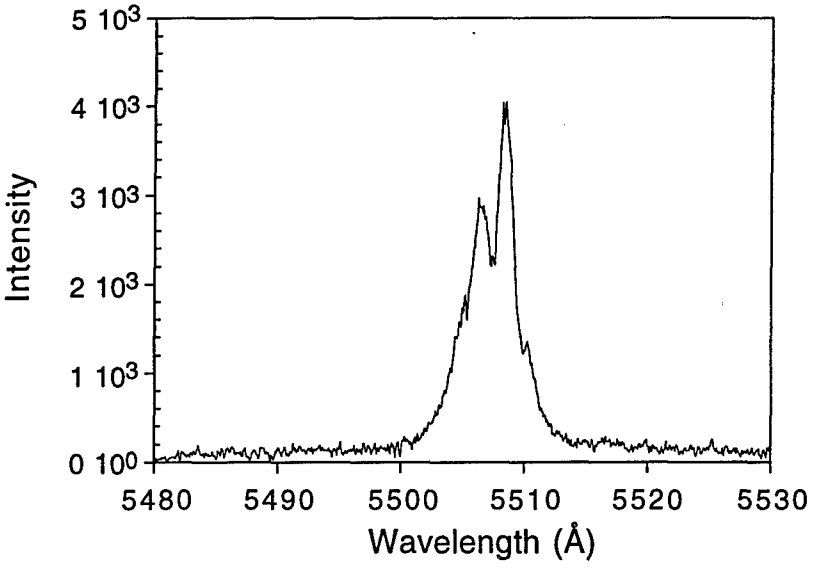

Figure 7 The 1284 cm^{-1} Raman feature of N_2O in supercritical water at 510 °C and 27.5 MPa.

when the collision partner is argon. This expression accurately represents their data measured over an experimental temperature range of 1000-1350 K. Evaluating this expression at 510 °C yields $k_{eff} = 1.5 \times 10^{-6}$ s^{-1}. We have measured this process in supercritical water by permitting N_2O to decompose over a 18 hour period at these conditions, and recorded a loss of N_2O of 77%. This corresponds to an effective first order rate constant of 2.3×10^{-5} s^{-1}. We note that Johnnson et. al. suggest that the presence water vapor can significantly enhance the decomposition rate of N_2O.

Data reported by others (Killilea, *et al.*, 1991) indicate that, in SCWO applications, N_2O is present in the gaseous effluent during the oxidation of NH_3 and other nitrogen containing species. However, the amount is small, and is observed to decrease significantly at higher temperature. Although there may be a noticeable increase in the decomposition rate in supercritical water relative to dry argon, the apparent thermal stability of N_2O represented by a still very slow thermal decomposition rate suggests that the N_2O consumption mechanism in SCWO applications must be due to its participation as an oxidant that competes very effectively with O_2 and oxidizing radicals for the fuel species in the reacting mixture.

This work was supported partly by the Sandia (SERDP) program and partly by the ARO URI (Army Research Office University Research Initiative) program.

Interlaboratory comparison of SCWO methanol kinetics

As highlighted in our last report, we have made several design changes to the MIT bench-scale reactor system in an effort to improve the agreement between the MIT and Sandia methanol oxidation data sets. The initial attempt to compare MIT and Sandia methanol data showed that under identical operating conditions Sandia consistently observed a higher conversion of methanol. Comparing the data on an assumed 1st-order Arrhenius plot reveals that the difference in the apparent rate corresponds to a potential temperature measurement mismatch between the reactors of approximately 15°C. As a result of this observation, we installed a new preheating system to improve our ability to preheat the oxidant and organic feeds prior to mixing at the reactor head. This change was made in response to our belief that we were losing heat in the transfer line between our preheater and the main sandbath. This heat loss, combined with a systematic thermocouple measurement error, led us to overestimate the true fluid temperature in our reactor.

The new preheating system consists of two 12-m lengths of coiled 0.11 cm ID (0.0625" OD x 0.01" wall) Hastelloy C-276 tubing. A voltage is applied across each of the preheaters, and the electrical resistance of each tube results in ohmic heating of the fluid stream flowing through it. This direct ohmic preheating approach allows us to fully preheat the organic and oxidant streams to reaction temperature (450 – 600°C). The temperature of each stream is controlled by an Omega CN9000A series PID temperature controller which sends a mA signal to a silicon controlled rectifier power supply, which in turn controls the number of voltage cycles applied across the preheater.

In November, Dr. Steven Rice of Sandia visited MIT for a period of two days. The purpose of the visit was to review the status of the comparative work, discuss the design of the two reactor systems, share experimental observations, and discuss a future course of action. The main result of this collaboration was an experimental plan for a series of methanol oxidation experiments that will be jointly performed by MIT and Sandia. An additional outcome of the meeting was Sandia's interest in examining the potential for axial temperature variations in their tubular reactor.

Kinetics of aromatics in supercritical water

Experimental work on aromatics in the tubular reactor will continue after the methanol comparison work is completed. We are using this opportunity to

enhance our analytical techniques for the identification of partial oxidation products from the SCWO of aromatics, including the detection of recombination products. An analytical method for the detection and quantification of cyclopentadiene, an anticipated partial oxidation product, which is observed in low-pressure combustion, is now in place. Dr. K.C. Swallow, an analytical chemist from Merrimac College, has agreed to provide assistance on the use of LC with diode-array detection and GC-MS techniques for product identification. Additionally, we have purchased a recirculation/refrigeration bath to stabilize samples for analysis and a GC sample tray which, too, will improve the reproducibility and quality of the GC analyses.

Hydrolysis of CH_2Cl_2 in sub- and supercritical water

Work has continued on the analysis of methylene chloride (CH_2Cl_2) hydrolysis data gathered earlier and the modeling of solvent effects. The focus has been to account for the significant reaction under subcritical conditions and very little reaction under supercritical conditions. The ultimate objective is to use the information gained from this work to generate a global rate expression for CH_2Cl_2 hydrolysis and oxidation in sub- and supercritical water.

As reported last time, the loss of polarity of water as it is heated through the critical point should have a debilitating effect on the ionic-based CH_2Cl_2 hydrolysis reaction because of the decreased stability of the polar transition state complex. This can quantitatively be accounted for through the use of a correction factor to the standard Arrhenius rate expression form given by a combination of Kirkwood and transition state theories. To calculate the correction factor, one needs to know the dipole moment (μ) and radius (r) of the two reactants and their transition state. We have been using *ab initio* electronic structure calculations to determine these two properties for these species. Thus far, the calculations continue to be in good agreement with what one would expect and with what we have observed experimentally; they do show a much higher μ or charge density for the transition state as anticipated and predict that the value of the rate constant at 550°C should drop by more than 8 natural log units due to the decreasing polarity of water under these conditions. The calculations now also reproduce the correct stereochemistry of the reaction and yield the expected location and structure of the transition state. Once this position of the transition state has been verified, we will use the corresponding values of μ and r in the correction factor along with our original experimental data to determine accurate global rate expressions by nonlinear regression.

Princeton University, Mechanical and Aerospace Engineering Department

Our project goal of describing the oxidation kinetics in supercritical water by forging a relationship to existing gas phase mechanisms has been successful for light alcohols and methane. At the time this work was initiated, there was already in place a considerable literature on these systems. However, the extension of this modeling strategy to aromatics required the development of accurate gas phase models in the intermediate temperature range. The research at Princeton has been directed at developing these lower pressure models as a starting point for SCWO model development.

As reported previously, reaction intermediate data from the oxidation of anisole ($T \sim 1000$ K) over a range of equivalence ratios ($\phi = 0.62 - 1.71$) was found not to differ substantially from anisole pyrolysis data. More specifically, yields of anisole, cresols, phenol, benzene, cyclopentadiene, methane, and ethane were independent of ϕ. Oxidation was found to occur preferentially through methylcyclopentadiene, accompanied by the production of CO and C_2–C_4 hydrocarbons including acetylene, ethene, allene, propene, methylacetylene, and 1,3-butadiene. These results suggest that 1) a model for the oxidation of anisole will rely heavily on the pyrolytic chemistry already developed and 2) extension of the pyrolysis model will involve primarily the addition of reaction steps describing the oxidation of methylcyclopentadiene.

Only two isomers of methylcyclopentadiene are observed experimentally but all three are present in the reacting system. 5-$CH_3C_5H_5$ is formed initially and is rapidly converted to 1-$CH_3C_5H_5$ which in turn is converted to 2-$CH_3C_5H_5$. Abstraction of an allylic H from any one of the three forms yields the same resonantly stabilized methylcyclopentadienyl radical. Addition of O or HO_2 to $CH_3C_5H_4$· yields an energized adduct which can decompose to lower energy, non-cyclic products by β-scission reactions. These radical recombination routes are outlined in Figure 8.

Recombination of HO_2 with $CH_3C_5H_4$· yields a methylcyclopentadienyl hydroperoxide that will rapidly dissociate either back to reactants or to a methylcyclopentadienyl-oxy radical and OH. This is likely one of the most important chain branching reactions; the OH product is more reactive than HO_2 and thus will accelerate the overall reaction via abstractions.

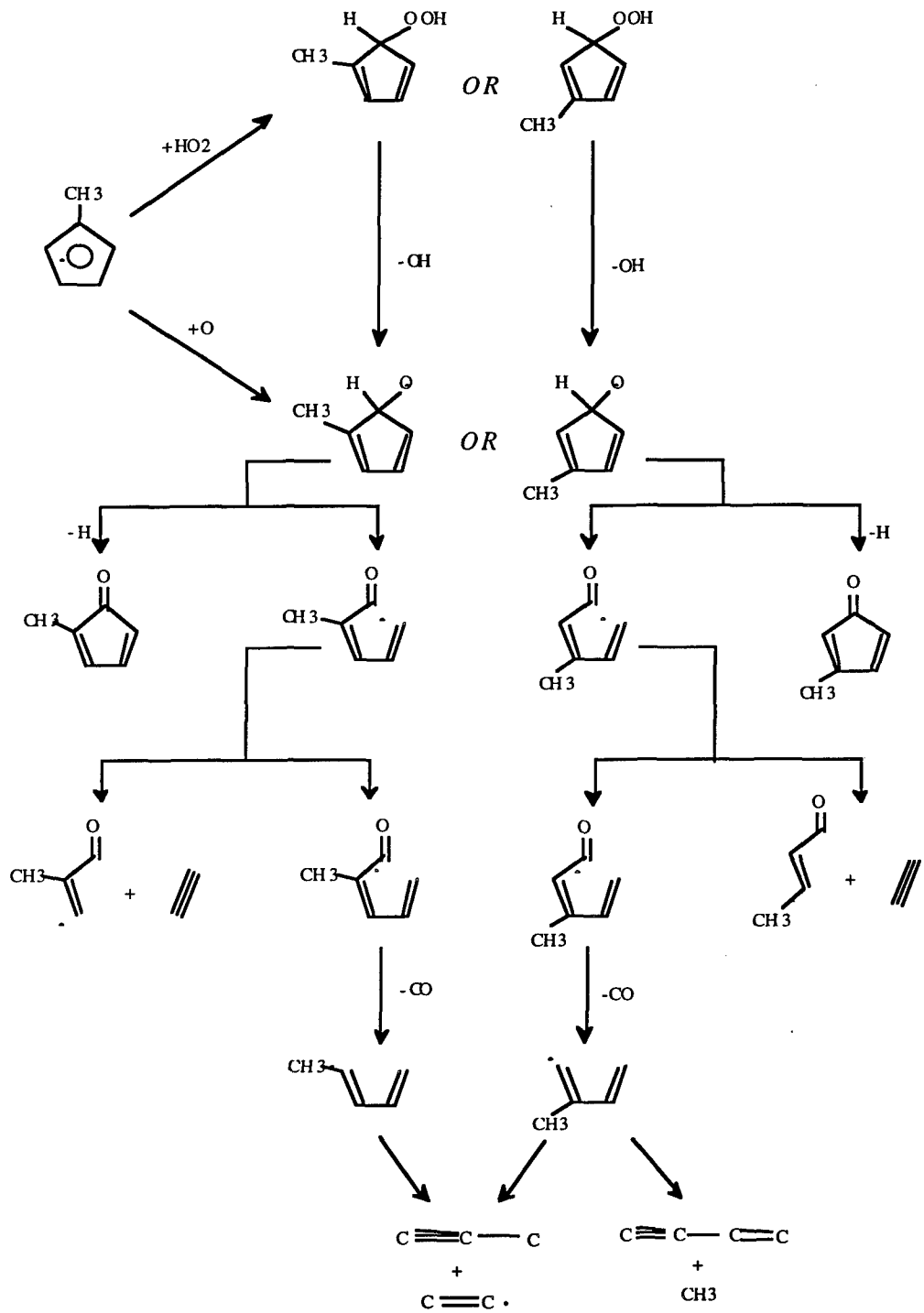

Figure 8 Methylcyclopentadiene oxidation mechanism showing the pathway to smaller hydrocarbons.

The methylcyclopentadienyl-oxy radical may also be formed directly by recombination of O atom with $CH_3C_5H_4$·. The radical will undergo rapid unimolecular dissociation near 700 °C via two low energy channels. One of these yields a methylcyclopentadienyl ketone and H atom. The second is a ring opening reaction to form a methylpentadienyl aldehyde radical. This radical may decompose to acetylene and a C_4 aldehyde radical, but is more likely to undergo rapid internal abstraction of the aldehydic hydrogen to form a more thermodynamically stable carbonyl radical. The carbonyl radical will decompose to CO and a C_5 hydrocarbon radical. The structure of this hydrocarbon radical is determined by the site at which the initial recombination (i.e. of O or HO_2 with $CH_3C_5H_4$·) took place; either the straight-chain 1,3-pentadien-4-yl radical or the branched 2-methyl-1,3-butadien-1-yl radical is formed. Subsequent reactions of these radicals yield C_2–C_4 species. The straight-chain pentadienyl radical undergoes β-scission to form methylacetylene + vinyl. 2-methyl-1,3-butadien-1-yl, a radical of isoprene, may decompose via two distinct β-scission channels to yield either methylacetylene + vinyl or vinylacetylene + methyl.

Allene may be formed via isomerization of methylacetylene. Recombination of vinyl with H, methyl, or vinyl yields ethene, propene, and 1,3-butadiene, respectively. Alternatively, vinyl may unimolecularly decompose to acetylene + H.

The scheme described above accounts qualitatively for C_2–C_4 methylcyclopentadiene oxidation products observed in the anisole experiments. Further development of this model will involve consideration of radical addition to unsaturated bonds of the parent species. As yet, measured rates and thermodynamic data for the relevant reactions and species do not exist, and development of a model for quantitative prediction must rely heavily on estimations. Recent advances in this laboratory in the modeling of the unsubstituted species cyclopentadiene are expected to aid in the present modeling effort.

A preliminary model for the oxidation of phenol has been developed which predicts well the fuel decay and the production of major species. Further refinement of estimated rates and thermodynamic data is underway.

References

Johnsson, J. E.; Glarborg, P.; Dam-Johansen, K. Thermal Dissociation of Nitrous Oxide at Medium Temperatures. Twenty Fourth Symposium (International) on Combustion, 1992, 917-923.

Killilea, W. R.; Swallow, K. C.; Hong, G. T. The fate of Nitrogen in Supercritical Water Oxidation. Second International Symposium on Supercritical Fluids, Boston, MA, 1991, 173-177.

INITIAL DISTRIBUTION

Dr. Merrill Heit, Jr.
U.S. Dept. Of Energy
19901 Germantown Rd.
Germantown, MD 20874

Dr. Robert Marianelli
U.S. Dept. Of Energy
19901 Germantown Rd.
Germantown, MD 20874

Dr. Paul Maupin
ER-142
U.S. Dept. Of Energy
19901 Germantown Rd.
Germantown, MD 20874

Dr. Robert W. Holst
SERDP Program Office
Program Manager for Compliance and
Global Environmental Change
901 North Stuart Street, Suite 303
Arlington, VA 22203

Mr. Ed Ansell
US Army Defense Ammunition
Center
Attn: SMCAC-TD
Savanna, IL 61074-9639

Ms. Jenny Dowden
Labat-Anderson Incorporated
8000 Westpark Dr.
Suite 400
McLean, VA 22102

Dr. Bradley P. Smith
SERDP Program Office
901 North Stuart Street, Suite 303
Arlington, VA 22203

Mr. Jim Hurley
US AF AL/EQS
139 Barnes Drive, Suite 2
Tyndall Air Force Base, FL 32403

Mr. Richard Kirts
Naval Civil Engineering Laboratory
560 Laboratory Dr.
Port Hueneme, CA 93043-4328

Mr. Crane Robinson
Arament Research
Development & Engineering Center
(ARDEC)
SMCAR-AES-P
Building 321
Picatinny Arsenal, NJ 07806-5000

Dr. Peter Schmidt
Office of Naval Research
Chemistry Division
800 North Quincy Street
Arlington, VA 22217-5660

Dr. Regina E. Dugan
DARPA/DSO
3701 N. Fairfax Dr.
Arlington VA 22203-1714

Dr. Robert Shaw
Chemical & Biological Sciences Div.
U.S. Army Research Office
Research Triangle Park, NC 27709-2211

Prof. Martin A. Abraham
Dept of Chem. and Environ. Eng.
University of Toledo
Toledo, OH 43606

Prof. Joan F. Brennecke
University of Notre Dame
Department of Chemical Engineering
Notre Dame, IN 46556

Dr. Kenneth Brezinsky
Dept. of Mechanical and Aerospace Engineering
Princeton University
PO Box CN5263
Princeton, NJ 08544-5263

Prof. Klaus Ebert
Kernforschungszentrum Karlsruhe
Institut fur Heisse Chemie
Postfach 3640
D-76021 Karlsruhe
Germany

Dr. Robert E. Huie
National Institute of Standards and Technology
Chemistry A261
Gaithersburg MD 20899

Prof. Earnest F. Gloyna
University of Texas at Austin
Environmental and Health Engineering
Austin, TX 78712

Prof. Keith Johnston
University of Texas at Austin
Chemical Engineering Dept.
26th and Speedway
Austin, TX 78712-1062

Prof. Micheal T. Klein
Chairman
University of Delaware
Chemical Engineering Dept.
Colburn Labs Academic Street
Newark, DE 19716-2110

Prof. Phillip E. Savage
University of Michigan
Chemical Engineering Department
Herbert H. Dow Building
Ann Arbor, MI 48109-2136

Prof. Jefferson W. Tester
Massachusetts Institute of Technology
Energy Laboratory
Room E40-455
77 Massachusetts Avenue
Cambridge, MA 02139

Mr K.S. Ahluwalia
Foster Wheeler Development Corporation
Engineering Science & Technology
12 Peach Tree Hill Road
Livingston, NJ 07039

Mr. Armand A. Balasco
Arthur D. Little Inc.
Acorn Park
Cambridge, MA
02140-2390

Dr. Joseph M. Cardito
Stone and Webster
245 Summer Street
Boston, MA 02210

Dr. Hiroshi Inomata
Tohoku University
Aoba Aramaki
Sendai 980
JAPAN

Mr. Thomas G. McGuinness
255 41st St.
Apt. 9
Oakland CA 94611

Dr. Carol A. Blaney
Kimberly-Clark
1400 Holcomb Bridge Rd.
Roswell, GA 30076-2199

Dr. David A. Hazelbeck
General Atomics
M/S 15-100D
3550 General Atomics Court
San Diego, CA 92121-1194

Dr. William Killilea
General Atomics
3550 General Atomics Court
San Diego, CA 92121-1194

Dr. Richard C. Lyon
Eco Waste Technologies
2305 Donley Drive
Suite 108
Austin, TX 78758-4535

Mr. Dan Greisen
1940 Alabama Ave
PO Bxo 3530
Rancho Cordova, CA 95741-3530

Dr. Steven J. Buelow
CST-6
Los Alamos National Lab.
Los Alamos, NM 87545

Dr. Philip C. Dell'Orco
Los Alamos National Laboratory
Explosives Technology & Safety C920
Los Alamos, NM 87545

Dr. Albert Lee
NIST
Bldg. 221 Room B312
Gaithersburg, MD 20899

Dr. William Pitz
LLNL
P.O. Box 808 L-014
Livermore, CA 94551-0808

Prof. Jean Robert Richard
CNRS
Combustion Laboratory
1C Avenue de la Recherche Scient.
Orleans 45071
France

Dr. Gregory J. Rosasco
Nat'l Institute of Standards and
Technology
Division 836, Bldg. 221, Rm B-312
Gaithersburgh, MD 20899

MS0828 P. J. Hommert, 1503

MS0701 R. W. Lynch, 6100
MS0735 D. E. Arvizu, 6200
Attn: 6203 A. P. Sylwester
6211 G. A. Carlson
6212 N. B. Jackson

MS0756 G. C. Allen, 6607

MS9001 T. O. Hunter, 8000
Attn: 8100 M. E. John
8200 L. A. West
8400 R. C. Wayne
8800 P. E. Brewer

MS9214 C. Melius, 8117

MS9054 W. J. McLean, 8300

MS9042 C. Hartwig, 8345

MS9051 L. Rahn, 8351

MS9055 F. Tully, 8353

MS9052 D. R. Hardesty, 8361 (2)

MS9052 S. W. Allendorf, 8361

MS9052 M. D. Allendorf, 8361

MS9052 L. L. Baxter, 8361

MS9052 S. G. Buckley, 8361

MS9052 M. M. Lunden, 8361

MS9052 T. A. McDaniel, 8361

MS9052 D. K. Ottesen, 8361

MS9052 C. Shaddix, 8361

MS9052 E. Croiset, 8361

MS9052 R. Hanush, 8361

MS9052 S. Rice, 8361 (20)

MS9053 R. Carling, 8362

MS9053 R. Steeper, 8362

MS9053 R. Gallagher, 8366

MS9101 B. Peila, 8411

MS9105 T. T. Bramlette, 8422

MS9105 J. Lipkin, 8419

MS9406 B. Haroldsen, 8412

MS9406 H. Hirano, 8412

MS9406 C. LaJeunesse, 8412

MS9406 M. C. Stoddard, 8412

MS9404 B. Mills, 8713